58916-00-105, 85088-24-105

ANL/MSD/PP--92032

From meandering to straight grain boundaries: Improving the structures of artificially-induced grain boundaries in superconducting $YBa_2Cu_3O_y$ bicrystals

X.F. Zhgang, V.R. Todt, and D.J. Miller

Materials Science Division and Science and Technology Center for Superconductivity
Argonne National Laboratory, Argonne, IL 60439

DISCLAIMER

Work supported by U.S. Department of Energy, Division of Basic Energy Sciences-Materials Sciences, and Energy Efficiency and Renewable Energy, as part of a DOE program to develop electric power technology, under contract #W-31-109-ENG-38; and by the National Science Foundation Office of Science and Technology Centers for Superconductivity under contract DMR #91-20000.

From meandering to straight grain boundaries: Improving the structures of artificially-induced grain boundaries in superconducting $YBa_2Cu_3O_y$ bicrystals

X.F. Zhang, V.R. Todt, D.J. Miller

Materials Science Division, and
Science and Technology Center for Superconductivity
Argonne National Laboratory, Argonne, Illinois 60439, U.S.A.

Abstract:

This paper presents several key aspects of our successful approach to preparing artificially-induced [001] tilt $YBa_2Cu_3O_y$ (YBCO) grain boundaries (GBs) with uniform, well-defined structures. We have compared the structure of GBs produced in thin film bicrystals and bulk bicrystals, respectively. In the YBCO thin film bicrystals prepared by off-axis magnetron sputtering, meandering rather than planar GBs were generally formed due to the three-dimensional island-shaped nucleation and growth of the thin films. Experimentally, using a low film deposition rate has been demonstrated to reduce the magnitude of meander. However, complete elimination of the meandering configuration has not yet been accomplished due to the film growth mechanism. Thus, we have developed a dual-seeded-melt-texture process to produce uniform, planar GBs in [001] tilt YBCO bulk bicrystals. Transmission electron microscopy (TEM) studies revealed GBs with a remarkably planar configuration on both micro- and nano-meter scales, demonstrating that simpler, meander-free GB microstructures with well defined [001] tilt angle have been successfully produced compared to those formed in bicrystal thin films. The high reproducibility, excellent stability and well controlled GB orientations have established the dual-seeded-melt-texture process as a reliable technique for engineering artificial GBs for the purpose of systematic studies of GB properties and allow for more insightful measurements of transport properties across individual GBs.

PACS: 61.72.Mm, 74.72.Bk
Keywords: Superconducting grain boundary, microstructure.

I. Introduction

The fabrication of high transition temperature (T_c) superconducting GBs with controlled microstructures is an important step in developing an improved understanding of GB transport properties. Various techniques for fabricating such GBs have been developed. One of the more common methods is to deposit epitaxial superconducting thin films on suitable bicrystal substrates. As an example, the geometry of an [001] tilt bicrystal is shown schematically in fig. 1. Epitaxial growth of the thin film on each half of such bicrystals yields an artificially-induced GB. Chaudhari et al. demonstrated that the critical current density (J_c) across artificial GBs formed in YBCO thin film bicrystals is always significantly less than that of either adjacent grains.[1] Dimos et al. and Ivanov et al. further demonstrated an inverse relationship between the J_c across the GB and the misorientation angle (θ) of the YBCO film bicrystals.[2,3] It has generally been assumed that the GB in the film will follow the straight GBs in underlying substrate bicrystals, and in these previous studies, a planar GB configuration with well-defined orientations was assumed and used as a reference for orientation when electric current and/or magnetic fields were applied for characterization of transport properties. However, recent TEM studies revealed a much more complicated GB configuration formed in YBCO thin film bicrystals. The GB planes are meandering rather than planar.[4-10] The deviation of the YBCO GB away from the underlying substrate boundary varies from a few tens to hundreds of nanometers. GB planes with twist components have been observed in addition to the meander.[7,8,10] Due to the fact that the current transport behavior is likely to vary for different GB segments,[7,8,10] an unambiguous correlation between the microstructure and global transport properties is difficult to attain. Thus, fabrication of a more well-defined planar GB is crucial for more insightful studies of transport behavior.

Structural characterization and J_c measurements have also been carried out for GBs formed in melt-textured YBCO superconductors.[11-13] Although faceted GBs have been observed,[14] the GBs formed in such bulk bicrystals are generally planar. However, the length

scale and misorientation angle (θ) of bicrystals are quite random and difficult to control. Systematic measurements of J_c versus θ are thus rather difficult to achieve. Therefore, the synthesis of artificially-induced GBs with well controlled GB plane orientations and less complicated microstructure over large scales (e.g. millimeter scale) should be the direction of the further efforts.

In this paper, we demonstrate two methods to achieve a remarkable improvement in the GB configuration of bicrystal samples: by using low film deposition rates and a dual-seeded-melt-texture process. The much less complicated microstructure achieved for [001] tilt YBCO GBs offers the possibility for improved interpretation of measurements and a better understanding of the superconducting behavior of individual grain boundaries.

II. Experimental

YBCO thin films were deposited on commercially available [001] tilt (nominal) $SrTiO_3$ bicrystals by off-axis magnetron sputtering or pulsed organo-metallic beam epitaxy (POMBE). The configuration and deposition parameters used to deposit the YBCO films have been described elsewhere.[10,15] For the dual-seeded-melt-texture process of [001] tilt YBCO GBs, $Nd_{1+x}Ba_{2-x}Cu_3O_x$ (Nd-123) single crystals were used as the seeds and the misorientation between two halves of the synthesized YBCO bicrystals were controlled by the orientation of the seeds. The microstructure of GBs may be affected by various process parameters during the solidification procedure.[16] Grain boundary J_c versus θ values,[16] and other properties[17] have been measured and discussed. For this work, TEM characterization on GBs were carried out using Philips CM30 and Jeol 4000EX transmission electron microscopes, operated at 200 kV and 400 kV, respectively.

III. Results and Discussions

3.1. Reducing the magnitude of meander for the GBs formed in YBCO thin film bicrystals.

GBs formed in the YBCO thin film bicrystals are typically meandering rather than straight. Fig. 2a shows a [001] bright-field image for a YBCO thin film deposited on a [001] tilt 24° $SrTiO_3$ bicrystal by MOCVD. Close inspection reveals that meandering GBs are actually composed of facet segments which are a few tens of nanometers in length. Similar meandering GBs have been observed in YBCO bicrystal thin films prepared by sputtering as shown in fig. 3 in which the meandering GB is composed of short facets marked by black dots. The scale of the facets is only a few tens of nanometers and the facet plane can vary as we have shown previously.[7,8,10] The different GB planes that arise as a result of the meandering configuration preclude the straightforward interpretation of transport properties across the GB. Therefore, efforts have been directed to reducing the magnitude of the meander.

It has been shown that the growth of YBCO thin films on $SrTiO_3$ substrates with a planar (001) surface initiates with three-dimensional island-shaped nuclei heterogeneously distributed on the substrate surface.[18,19] Film growth proceeds via the Volmer-Weber growth mechanism in which each island grows independently and eventually coalesces with others to form the film. On the surface of the [001] tilt $SrTiO_3$ bicrystal substrate, the YBCO islands near the substrate GB may overgrow that boundary despite the very different orientation on the other side due to the bicrystal geometry. In principle, this overgrowth ability is the same for YBCO islands in either half of the bicrystal. Meandering GBs are thus formed between overgrown islands as illustrated schematically by fig. 2b. This formation mechanism for the meandering GB is supported in fig. 2a in which some islands are visible such as those marked by A and B (island A is also outlined by black dots). Based on this mechanism, meandering YBCO GBs are likely to form and have been observed in thin film bicrystals produced by a variety of techniques such as sputtering,[4-6,8,10] laser ablation[4,9] and POMBE[8] (fig. 2a). However, it is possible to have some degree of control over the meandering configuration by adjusting the film deposition conditions. The idea is based on the fact that the meandering shape is closely related to two factors: island size and overgrowth of islands across the substrate GB (fig. 2b), each of which in turn can be influenced by changing film deposition conditions. In our previous papers, we have demonstrated that the

magnitude of the meander in terms of amplitude and wavelength can be reduced by lowering the film deposition rate.[7,8,10] For example, a decrease of ~35 % in meander amplitude has been achieved by lowering the film deposition rate by a factor of 2.5 for [001] tilt 36.8° GBs in YBCO thin film bicrystals.[10] We attributed this reduction in roughness to a growth state approaching a more thermodynamically stable configuration.[7,8,10]

Although we have been able to effect a substantial reduction in the magnitude of the meanders by controlling the deposition rate, we have not yet been successful in completely eliminating the meandering configuration in YBCO thin film bicrystals. In our previous studies, we have shown that the spatial distribution of nucleation sites plays a role on the magnitude of the meander and that the lateral growth and coalescence of islands result in grain boundaries that may be decorated with secondary phases and impurities.[7,8,10] On the basis of these concepts, we developed a technique based on dual-seeded-melt-textured growth in an attempt to produce planar grain boundaries in YBCO **bulk** bicrystals.

3.2. Planar YBCO GBs prepared by dual-seeded-melt-texture process.

The scheme of dual-seeded processing is depicted in fig. 4. Nd-123 single crystals which have higher melting point than that of YBCO but a similar structure and lattice parameters as those of YBCO are chosen as seeds for melt-texture growth of YBCO bulk crystals. As illustrated in fig. 4, two Nd-123 single crystals are intentionally positioned in a way that their **c**-axes are parallel but a rotation is applied in the (**a-b**) planes. Two YBCO bulk crystals are formed by melt-textured growth, initiating from the two seed crystals respectively. The bicrystal is formed as the two domains merge with the misorientation angle determined by the misorientation between the two Nd-123 seeds. In principle, YBCO GBs with any desired [001] tilt angle can be prepared by this method because the misorientation angle between the two seeds can be controlled quite accurately with the aid of an optical microscope. Detailed processing procedures and parameters have been published elsewhere.[16]

TEM studies showed some similar structural features between [001] tilt YBCO GBs formed in bulk bicrystals and in thin film bicrystals. For example, twist GB planes and precipitates on GBs have been observed in both cases. Similar to the thin film bicrystal GBs,[8,10] the GB planes formed in bulk bicrystals were not always found parallel to the common **c**-axis but contain a twist component in some GB segments. The inclined GB planes result in a projected width along the **c**-axis as revealed by fig. 5, in which GB formed in a 18.5° bicrystal presents a variable projected width, indicating a twist GB plane in this segment. Twist components have also been observed in bulk bicrystals with other misorientation angles. This twist component can be understood as a consequence of a lateral growth of the YBCO due to the slower **c**-direction growth than **a**-direction (or **b**-direction) growth.[10] In fig. 5, a Y_2BaCuO_y (211) particle was trapped in the GB, but this was rarely observed in GB segments referred to 'clean GBs' in our previous paper.[16] It should be noted that in the 'clean' part of the GB, 211 particles and other impurities do not segregate preferentially to the GB as is common in thin film GBs.

The most remarkable feature for GBs produced by the dual-seeded-melt-texture process is the planar configuration on both the micrometer and nanometer scales for almost all GB angles. Fig. 6 shows a comparison in morphology between [001] tilt GBs formed in a 36.8° thin film bicrystal and in a 18.5° bulk bicrystal. In contrast to the meandering configuration for the GB in fig. 6a, the well defined and planar GB on a scale over 1 μm is quite spectacular in fig. 6b. Although some deviations from planarity do exist (right part of fig. 6b), the GB plane changes only slightly. On the scale of the meanders in the thin film bicrystal, the GB in the bulk bicrystal can be considered planar. Optical and scanning electron microscopy further showed that such GB planes remain essentially planar even on the millimeter scale.[16]

Fig. 7a and 7b present lattice-fringe and atomic images, respectively, for the 18.5° GB. The GB appears to be planar on the atomic scale although steps on the order of one or two unit cells in the (001) plane can exist along the GB. The orientation of the GB plane is well defined everywhere and in this case is 10° away from the symmetric position. Thus, in contrast to the

meandering YBCO GBs formed by depositing films on bicrystal substrates, a much simpler GB microstructure with overall planar configuration and well defined [001] tilt angle have been successfully produced. The high reproducibility and very simple GB microstructure over large scales can facilitate the investigations on physical behavior of individual YBCO GB.

It should be pointed out that although GBs formed by the dual-seeded-melt-texture process are often straight over large scales, GBs composed of long facet segments (a few hundred nanometers to microns in length) have been encountered also. Fig. 8 shows a bright-field image of a 4° YBCO bulk bicrystal. The bicrystal GB is marked with white dots and labeled "G.B.". The projected width observed for the GB indicates a twist component for GB plane as was shown in fig. 5. In fig. 8, the YBCO GB is not always straight but composed of facets with very different indices. The facet indices marked in fig. 8 refer to orientation 1 and orientation 2 in two halves of the bicrystal. In this case, the longest GB segment corresponds approximately to a $(010)_1/(010)_2$ facet. Some other short facets have also assumed this $(010)_1/(010)_2$ GB plane. A sharp deviation of the GB plane results in a change of the GB plane to approximately $(\bar{1}10)_1/(\bar{1}10)_2$ which is followed by another facet indexed as $(\bar{1}20)_1/(\bar{3}50)_2$. It should be pointed out that low index planes have been used in describing these facets in order to provide a clearer description. In fact, there exist small deviations of 3° and 1° from these low index planes for orientation 1 and orientation 2, respectively, such that the specific identity of the facet plane is of a higher index but very close to those shown in fig. 8. For example, $(\bar{1}10)_1$ marked in fig. 8 is actually an approximation of $(\bar{9}\ 10\ 0)_1$.

In fig. 8, the contrast observed within the grains corresponds to twins with twinning planes parallel to the (110) or $(\bar{1}10)$ lattice planes of YBCO. In addition, sub-boundaries and anti-phase domain boundaries are also observed. Two sub-boundaries (S.G.) are marked by dashed lines in fig. 8 and anti-phase domain boundaries have also been observed in the same sample. These sub-boundaries and anti-phase domain boundaries take place in two halves of the YBCO bicrystal and those near the bicrystal GB could influence the GB orientation. Therefore it

is not surprising to see the pronounced bending of the GB planes associated with sub-boundaries (fig. 8) or anti-phase domain boundaries. The GB facets which deviate significantly from the original direction may not be in the low energy configuration so that strain-field exists along these facets, resulting in rough edges of the $(\bar{1}10)_1/(\bar{1}10)_2$ and the $(\bar{1}20)_1/(\bar{3}50)_2$ facets as shown in fig. 8.

3.3. Less complication in microstructure, better understanding in physics.

The very different configuration between the two types of GBs discussed here (fig. 6) should be considered when grain boundary properties are discussed. One effect of the meandering configuration as observed in thin films is that the length of the GB probed during transport measurements is typically longer than the width of the microbridge W (see fig. 9). A factor of as large as 1.5 was measured in case of the boundary shown in fig. 6, in spite of the fact that the magnitude of meander has already been reduced in this case by using a lower film deposition rate. Due to the uniformity of the meandering configuration, this factor is not expected to change appreciably if measured over a larger distance (a few to tens of microns) typical for microbridges used for transport measurements. In addition, the proposed variation of transport properties as a function of the grain boundary plane[10,20] complicates this effect since some of the deviation facets contained in meander may support a lower J_c than the nominal GB plane whereas others may carry a higher J_c. Thus the effect of these deviations cannot be accounted for nor can they be controlled effectively. As a consequence, the J_c value determined from transport measurements across meandering GBs may not be accurate. Also, short facets contained in meandering GBs and the potential influence of the substrate[21] could lead to additional uncertainties in the measurement results. Meandering GB planes may also influence normal state properties of the GB[17] and complicate wave function determination for electron pairs. Therefore, the planar GBs produced by the dual-seeded-melt-texture process could result in a more convincing and clearer interpretation for transport properties of individual GBs.

Although facets and 211 particles are occasionally observed on the [001] tilt GBs formed in bulk bicrystals (fig. 5 and fig. 8), generally planar, clean GBs with well defined GB orientations are reproducibly available by the dual-seeded-melt-texture process. In addition, the properties of these bulk bicrystals have been found to be stable over a six-month period under ambient conditions,[17] in contrast to the gradually degraded properties of thin film bicrystals. Although J_C is generally lower in bulk crystals than in thin films, the present simple and planar GBs in bulk bicrystals provide a promising advancement for a good understanding in physics. For example, our data of J_C versus θ showed that J_C across GBs with θ less than 10^o is about two orders of magnitude higher than that across GBs with θ larger than 20^o, with a transition for GBs with θ between 10^o and 20^o. These results are significant because the well-defined, planar GBs in the bulk bicrystals, together with the absence of additional effects from an underlying substrate and secondary phase impurities suggest that this decrease in J_C is associated only with the misorientation and not external facets. In other words, the decrease in J_C with increasing θ is not due to extrinsic factors but an intrinsic feature of the [001] tilt YBCO bicrystal GBs. Presumably, the increased misfit dislocation density and varied bond configurations at GBs are responsible for the decrease in J_C.

VI. Summary

In the attempts to fabricate superconducting GBs with less complicated structures, we have used TEM to directly image and compare the microstructures of artificially-induced GBs formed in [001] tilt YBCO bicrystals. Although decreasing the film deposition rate has been demonstrated to be effective to reduce the magnitude of meander for GBs formed in YBCO thin film bicrystals, we have not yet been able to completely eliminate meandering configuration because of the film growth mechanism. However, planar GBs which are much less complicated in microstructure on both the micro- and nano-meter scales can be successfully formed in melt-textured YBCO bicrystals initiated from two misoriented Nd-123 single crystal seeds. This type of artificially-induced grain boundary is leading to a good understanding of transport behavior for individual GBs. The reproducibility, excellent stability and well controlled GB orientations

establish the dual-seeded-melt-texture process as a reliable technique for engineering artificial GBs useful for the systematic study of GB properties.

Acknowledgment

This work was partially supported by the National Science Foundation Office of Science and Technology Centers under contract DMR 91-20000 and by the U.S. Department of Energy, Basic Energy Sciences-Materials Sciences, and Energy Efficiency and Renewable Energy, under contract #W-31-109-ENG-38.

References

1. P. Chaudhari, J. Mannhart, D. Dimos, C.C. Tsuei, J. Chi, M.M. Oprysko and M. Scheuermann, Phys. Rev. Lett. **60**, (1988) 1653.

2. D. Dimos, P. Chaudhari, J. Mannhart and F.K. LeGoues, Phys. Rev. Lett. **61**, 219 (1988).

3. Z.G. Ivanov, P.A. Nilsson, D. Winkler, J.A. Alarco, T. Claeson, E.A. Stepantsov and A.Ya. Tzalenchuk, Appl. Phys. Lett. **59**, (1991) 3030.

4. C. Traeholt, J.G. Wen, H.W. Zandbergen, Y. Shen, J.W.M. Hilgenkamp, Physica C **230**, 425 (1994).

5. B. Kabius, J.W. Seo, T. Amrein, U. Dahne, A. Scholen, M. Siegel, K. Urban and L. Schultz, Physica C **231**, 123 (1994).

6. J.W. Seo, B. Kabius, D. Dahne, A. Scholen and K. Urban, Physica C **245**, 25 (1995).

7. D.J. Miller, D.G. Steel, F. Yuan, J.D. Hettinger, K.E. Gray, J. Talvacchio and J.H. Kang, Proceedings of The 1995 International Workshop on Superconductivity, June 18-21, Maui, Hawaii, U.S.A.

8. D.J. Miller, T.A. Roberts, J.H. Kang, J. Talvacchio, D.B. Buchholz and R.P.H. Chang, Appl. Phys. Lett. **66**, 2561 (1995).

9. J.A. Alarco, E. Olsson, Z.G. Ivanov, D. Winkler, E.A. Stepantsov, O.I. Lebedev, A.L. Vasiliev, A.Ya. Tzalenchuk and N.A. Kiselev, Physica C **247**, 263 (1995).

10. X.F. Zhang, D.J. Miller and J. Talvacchio, J. Mater. Res. **11** (1996) 2440.

11. S.E. Babcock, X.Y. Cai, D.L. Kaiser and D.C. Larbalestier, Nature **347**, (1990) 167.

12. M.B. Field, X.Y. Cai, S.E. Babcock and D.C. Larbalestier, Trans. on Appl. Superconduc. **3**, (1993) 1479.

13. C. Sarma, G. Schindler, D.G. Haase, C.C. Koch, A.M. Saleh and A.I. Kingon, Appl. Phys. Lett. **64**, (1994) 109.

14. I-Fei Tsu, S.E. Babcock and D.L. Kaiser, J. Mater. Res. **11**, 1383 (1996).

15. J. Talvacchio, M. G. Forrester, J. R. Gavaler, and T. T. Braggins, "YBCO and LSCO Films Grown by Off-Axis Sputtering," in Science and Technology of Thin Film Superconductors II, edited by R. McConnell and S. A. Wolf (Plenum, New York, 1990), pp. 57-66.

16. V.R. Todt , X.F. Zhang, D.J. Miller, Appl. Phys. Lett. **69** (24), (1996).

17. M. St. Louis-Weber, V.P. Dravid, V.R. Todt, X.F. Zhang, D.J. Miller and U. Balachandran, Phys. Rev. B, in press.

18. D.P. Norton, D.H. Lowndes, X.Y. Zheng, S. Zhu and R.J. Warmack, Phys. Rev. B **44**, 9760 (1991).

19. X. Zhu, G.C. Xiong, R. Liu, Y.J. Li, G.J. Lian, J. Li and Z.Z. Gan, Physica C **216**, 153 (1993).

20. S.E. Babcock and J.L. Vargas, Annu. Rev. Mater. Sci. **25**, 193 (1995).

21. D.H. Kim, D.J. Miller, J.C. Smith, R.A. Holobopp, J.H. Kang, and J. Talvacchio, Phys. Rev. B **44**, 7607 (1991).

Figure captions.

Fig. 1: Schematic drawing of a [001] tilt bicrystal. A grain boundary (GB) is formed between two crystals with exactly the same structure but a tilt about the common [001] direction. The (100) lattice planes in two halves of the bicrystal are shadowed.

Fig. 2: (a) Bright-field image taken along the [001] direction of the YBCO thin film bicrystal ($\theta = 24^o$) which was prepared by POMBE. The straight GB in the underlying substrate is marked by a line. The meandering GB formed in the YBCO film is indicated by an arrow. Letters A and B mark two visible islands and island A is outlined by black dots. Note the contribution of islands A and B to the formation of the meandering GB. (b) Schematic illustration for the formation mechanism of a meandering GB in a thin film bicrystal. Only islands around the substrate GB are drawn.

Fig. 3: [001] lattice-fringe images taken for the 36.8° GB formed in a [001] tilt YBCO thin film bicrystal. Short facet segments are marked by black dots.

Fig. 4: Scheme illustrating the formation of [001] tilt YBCO GBs by the dual-seeded-melt-texture process.

Fig. 5: HREM image of the 18.5° GB in the bulk bicrystal. Note the varied projected width of the GB. A 211 particle was trapped in the GB area.

Fig. 6: (a) Morphology of a 36.8° GB formed in the [001] tilt YBCO **thin film** bicrystal. A meandering GB was formed between two halves of the bicrystal which show darker and brighter image contrast, respectively, under the imaging conditions used. (b) Planar GB formed in a 18.5° [001] tilt YBCO **bulk** bicrystal. The same length scale is used for (a) and (b).

Fig. 7: (a) [001] lattice-fringe image and (b) atomic image showing the planar GB in the 18.5° bulk bicrystal.

Fig. 8: Bright-field image showing a faceted GB formed in a YBCO bulk bicrystal ($\theta = 4^o$). Orientations in two halves of the bicrystal are indicated and the subscripts 1 and 2 refer to the orientation 1 and orientation 2 of the bicrystal. Three relatively large GB facets are marked by white dots and indexed. Approximation in indexing GB facets is taken as pointed out in relative text of the paper. Short facets can be recognized on the $(010)_1/(010)_2$ GB plane as presented by a zig-zag line. The contrast within the crystals is due to twins. Two sub-boundaries are marked by S.B. and dashed lines. Note the large deviation of the bicrystal GB at the intersection with a sub-boundary (lower part of the figure).

Fig. 9: Schematic illustration of a microbridge patterned across a meandering GB formed in a thin film bicrystal. The width (W) of the microbridge is marked by a dashed line. Note that the GB length covered by the microbridge may be longer than W. A factor of 1.5 is measured according to fig. 6.

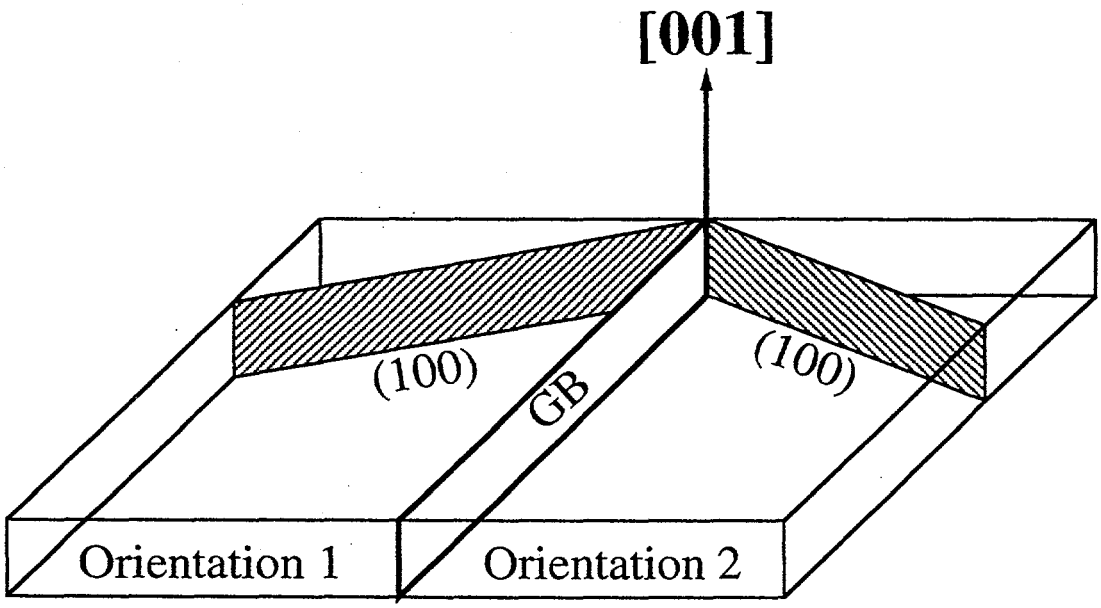

Schematic drawing of a [001] rotate bicrystal

Fig. 1
X.F. Zhang et al.

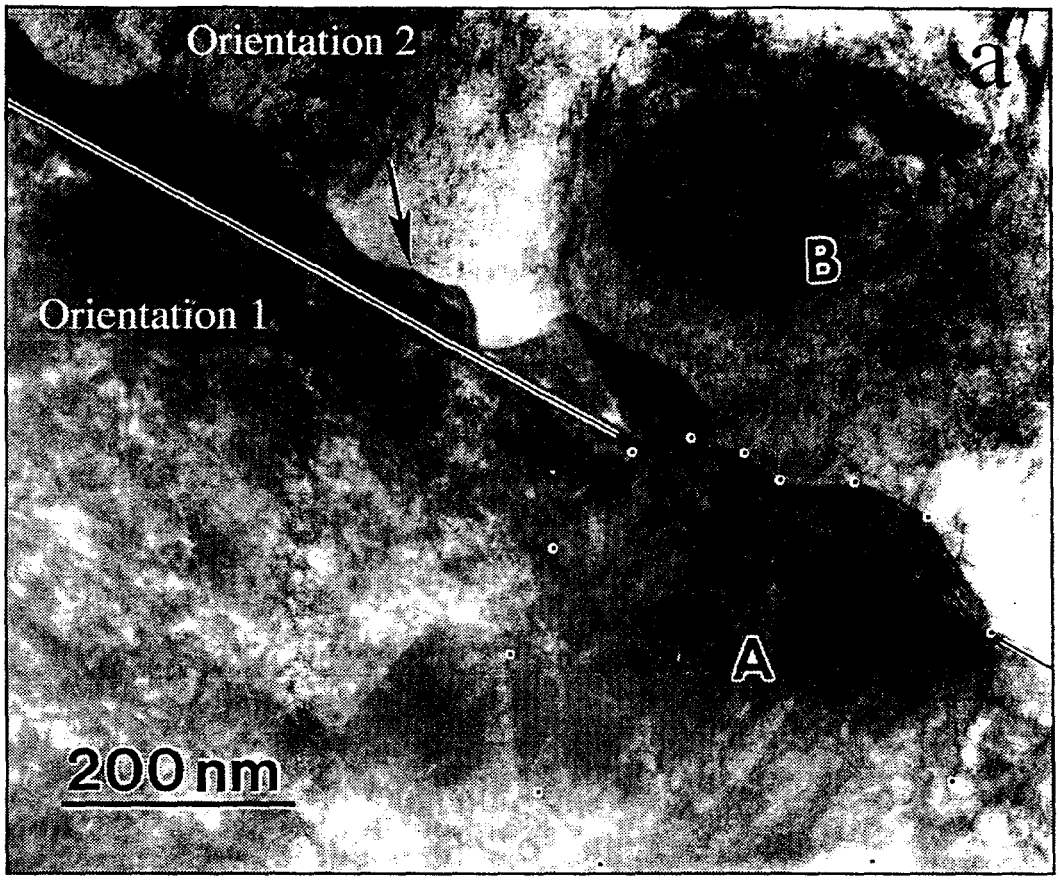
Orientation 2
a
B
Orientation 1
A
200 nm

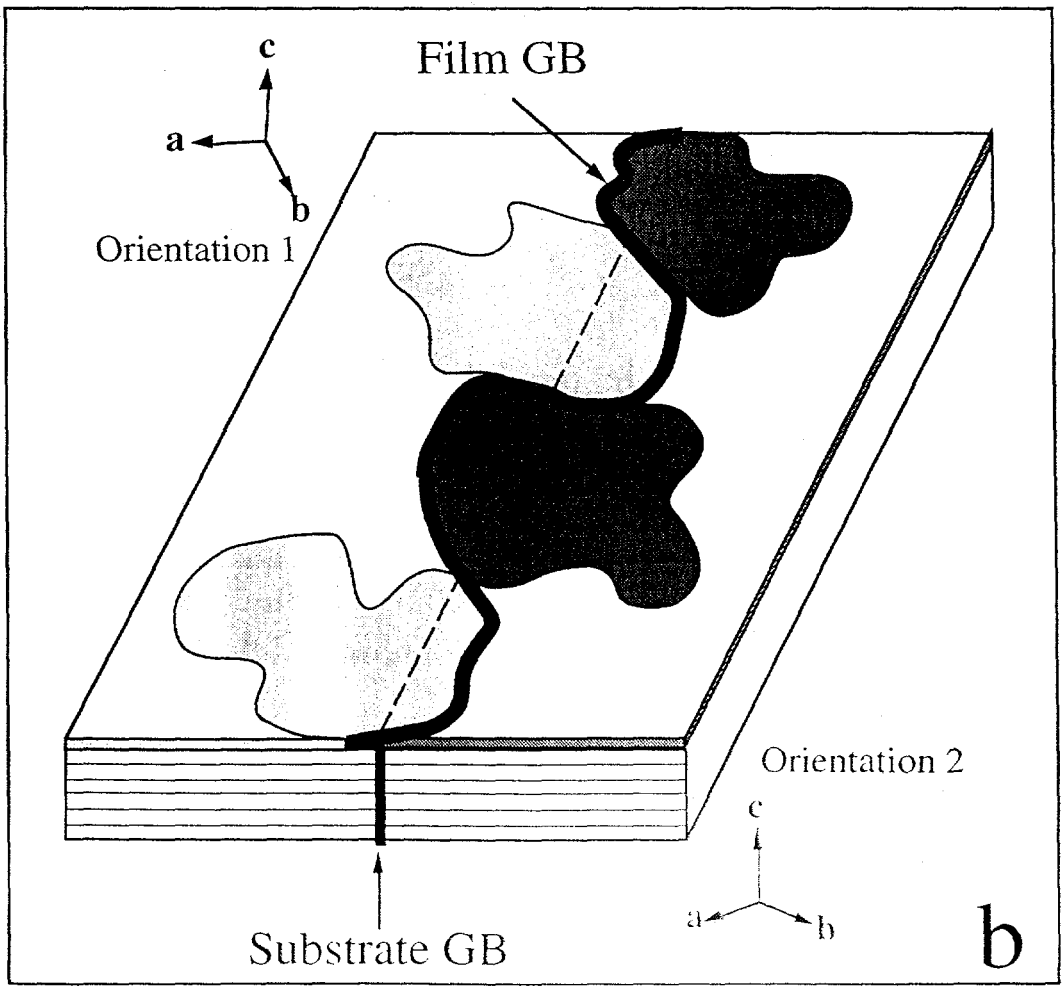
c
a
b
Film GB
Orientation 1
Orientation 2
c
a
b
Substrate GB
b

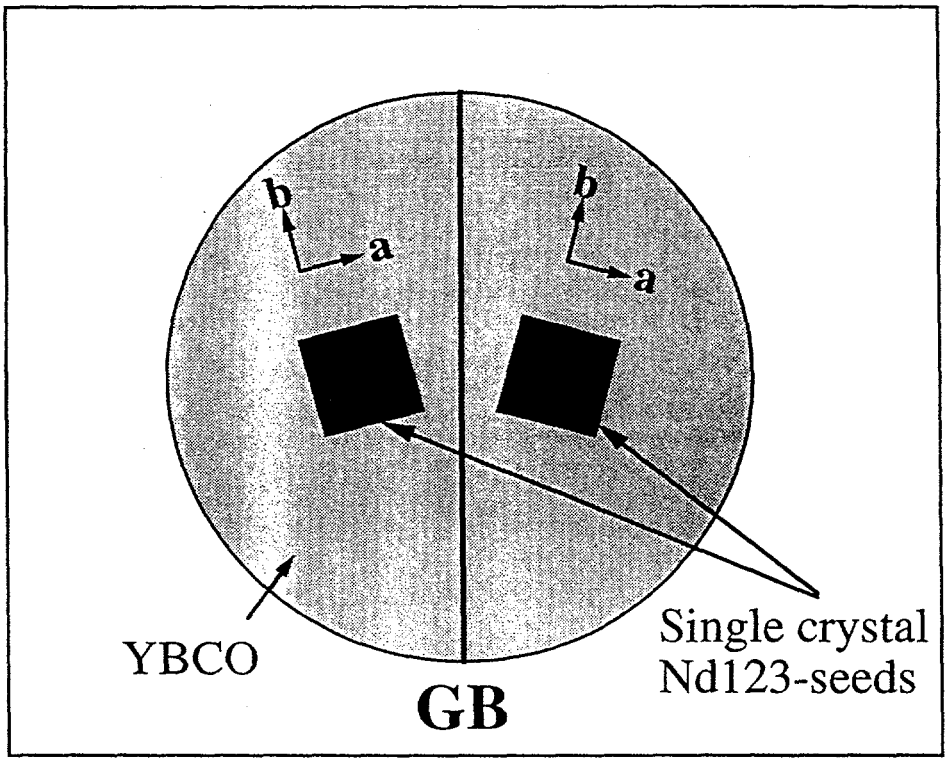

Fig. 4
X. F Zhang et al.

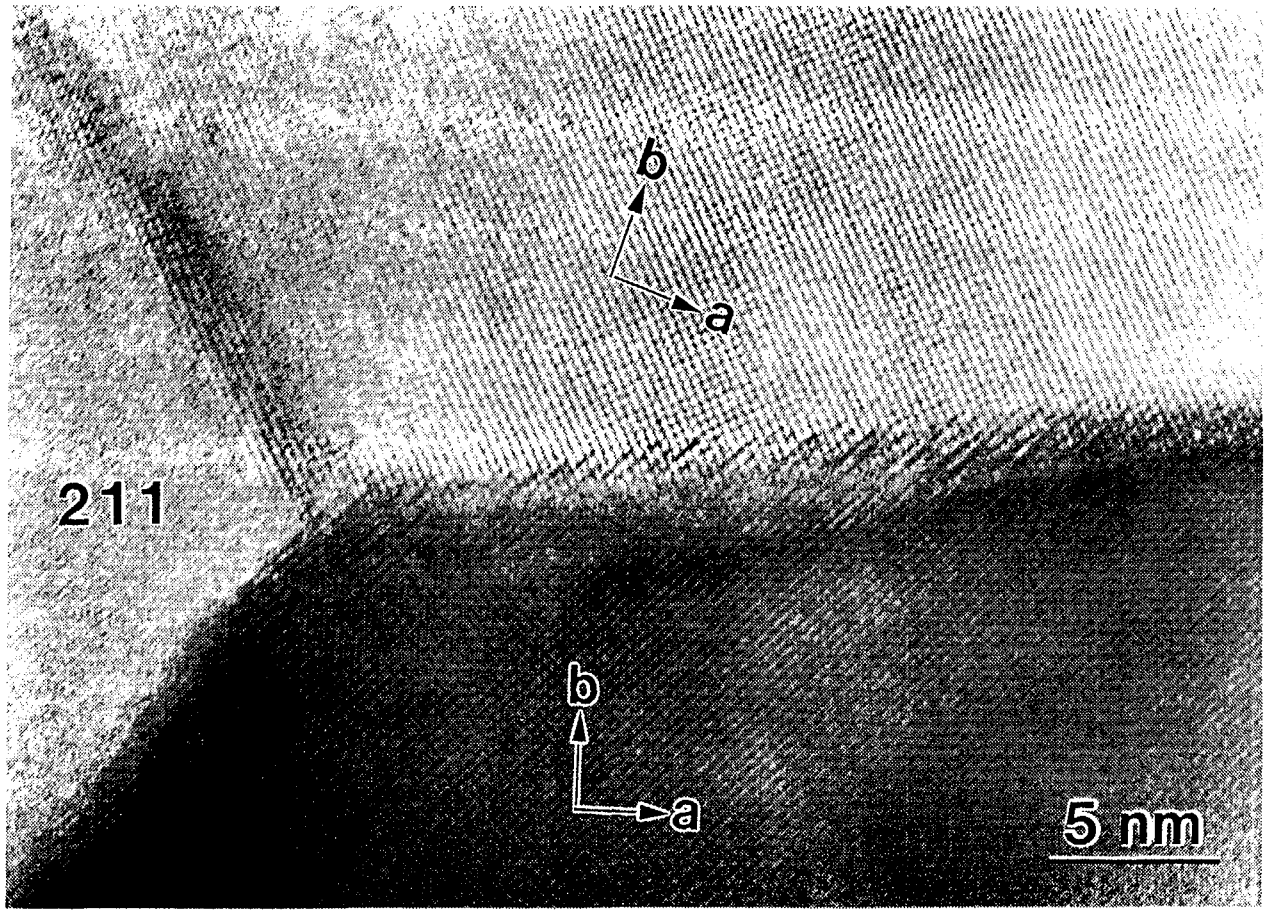
b
a
211
b
a
5 nm

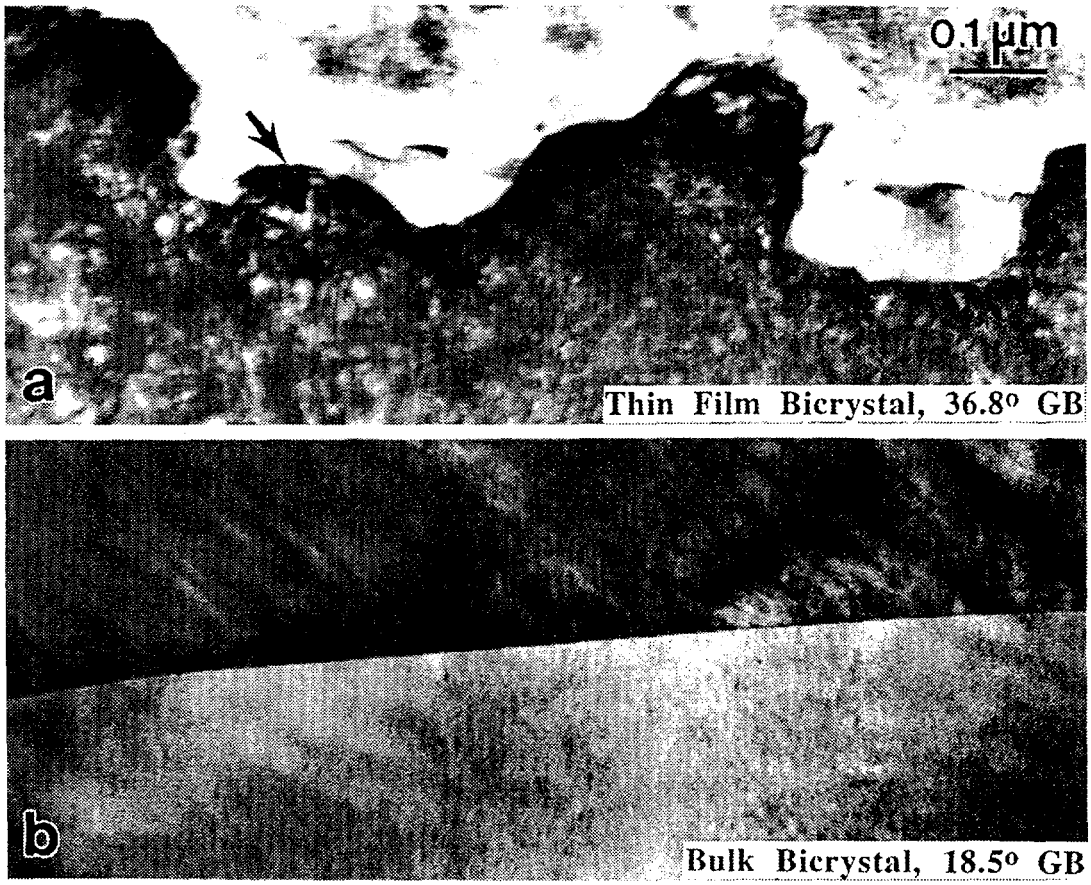
0.1 μm
a
Thin Film Bicrystal, 36.8° GB
b
Bulk Bicrystal, 18.5° GB

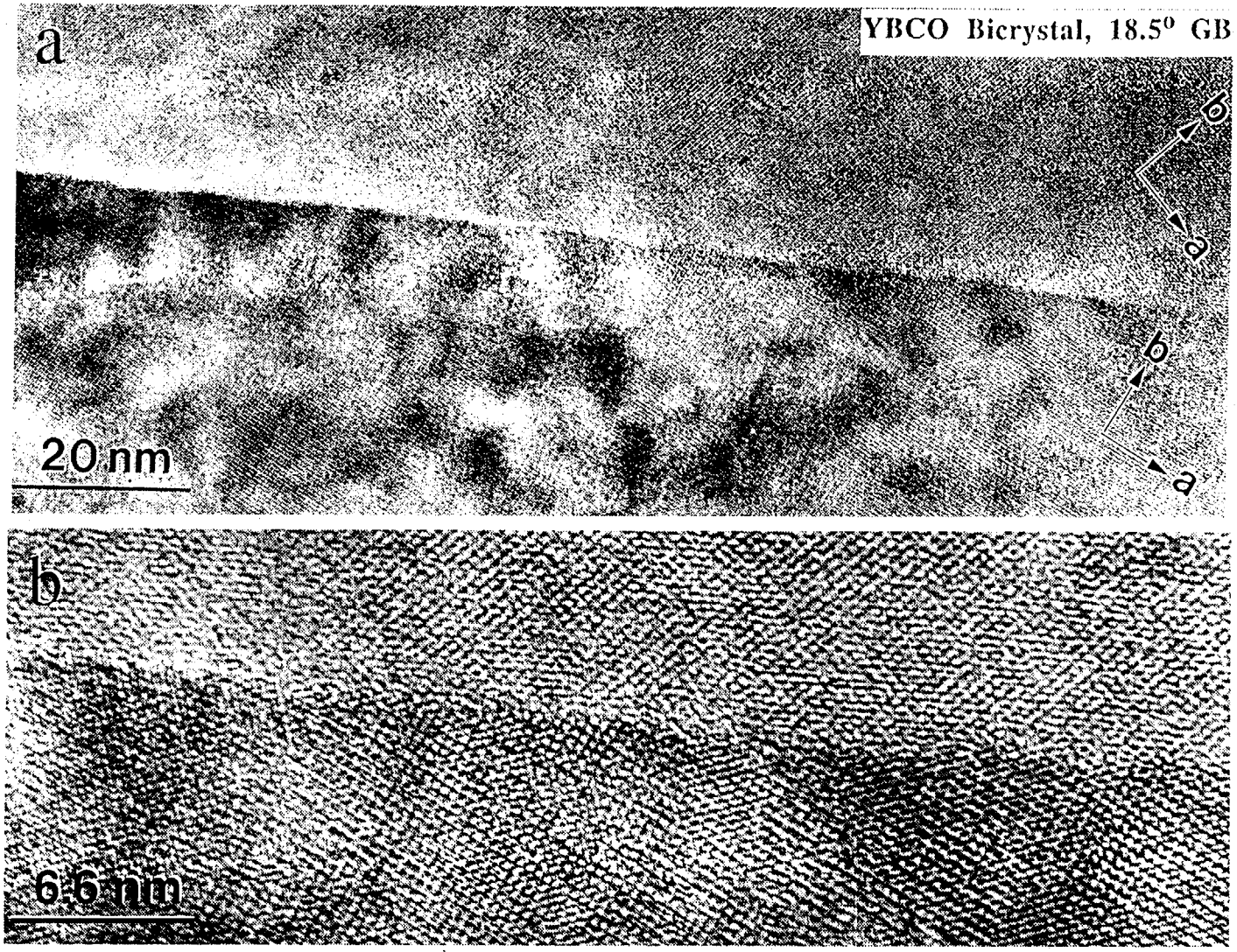
a
YBCO Bicrystal, 18.5° GB
b
a
b
a
20 nm
b
6.6 nm

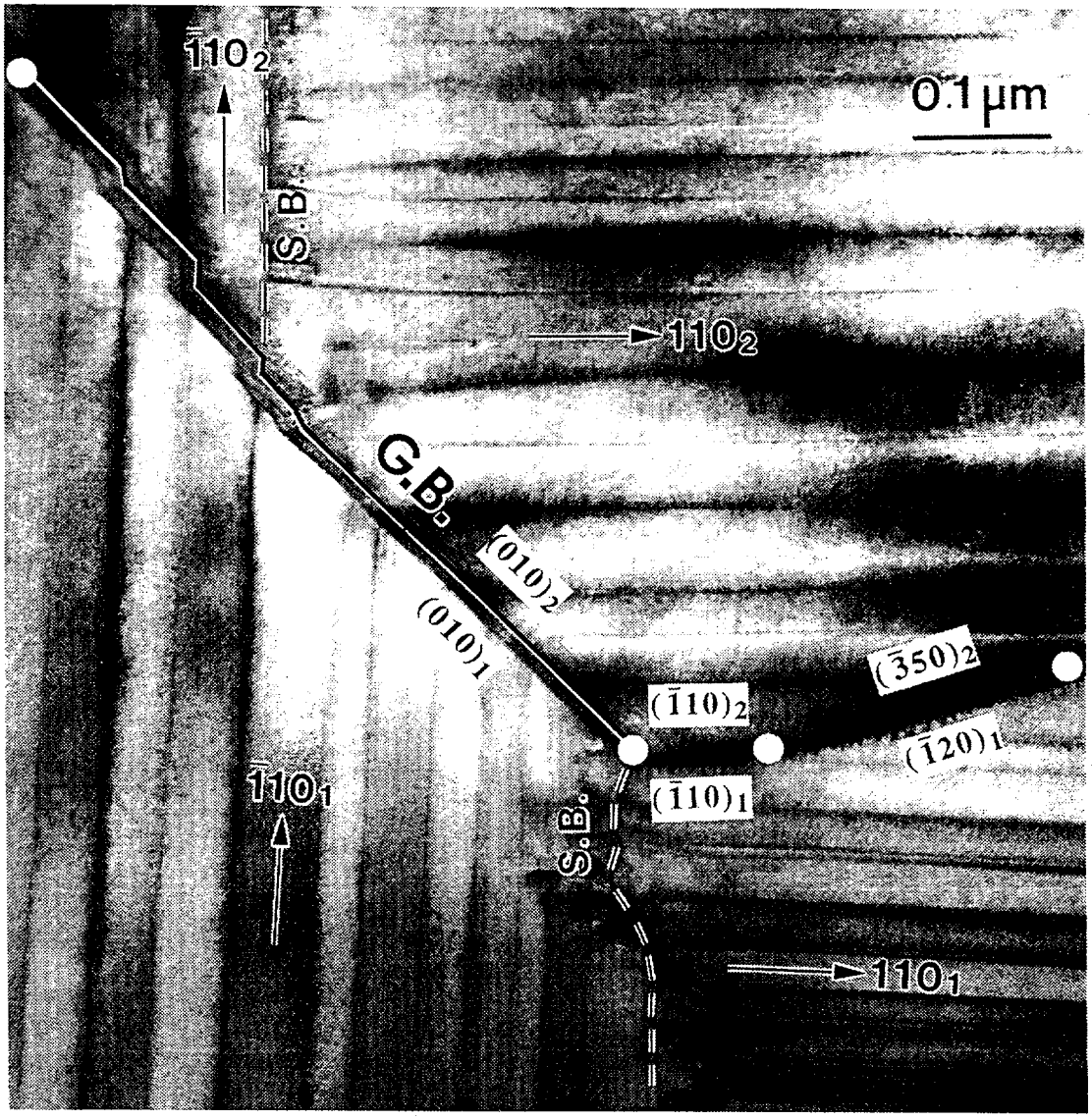
$\bar{1}10_2$
0.1 μm
S.B.
110_2
G.B.
$(010)_2$
$(010)_1$
$(\bar{3}50)_2$
$(\bar{1}10)_2$
$(\bar{1}20)_1$
$\bar{1}10_1$
$(\bar{1}10)_1$
S.B.
110_1

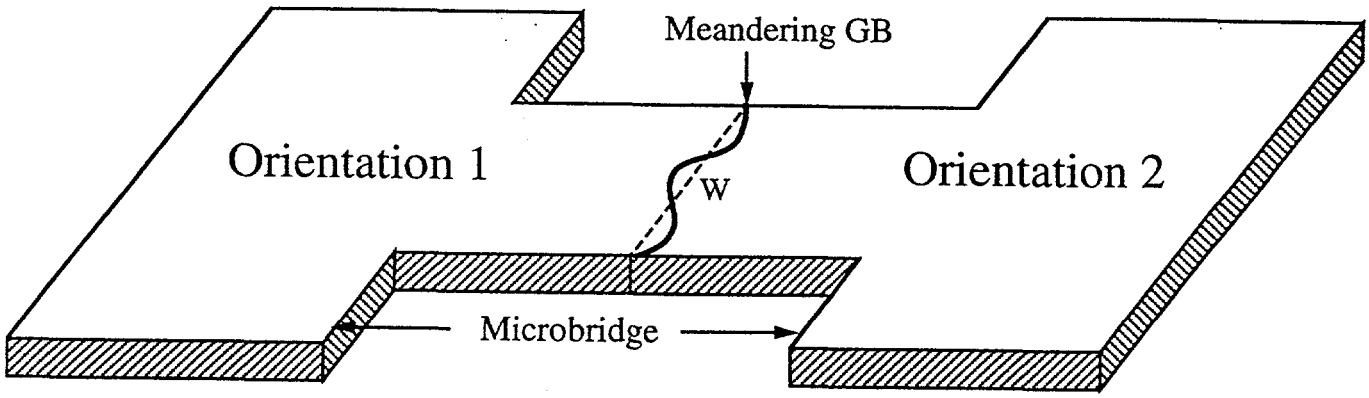

Fig. 9

X. F. Zhang et al.